X-33 ASCENT FLIGHT CONTROLLER DESIGN BY TRAJECTORY LINEARIZATION — A SINGULAR PERTURBATIONAL APPROACH

J. Jim Zhu and Brad D. Banker
Electrical and Computer Engineering Department
Louisiana State University
zhu@rsip.lsu.edu, bbanker@rsip.lsu.edu

Charles E. Hall
Vehicle and Systems Development Department
Control Systems Group
NASA Marshall Space Flight Center

An Extended Abstract
Submitted to
The 2000 AIAA GN&C Conference
As an Invited Session Paper

Abstract

The flight control of X-33 poses a challenge to conventional gain-scheduled flight controllers due to its large attitude maneuvers from liftoff to orbit and reentry. In addition, a wide range of uncertainties in vehicle handling qualities and disturbances must be accommodated by the attitude control system. Nonlinear tracking and decoupling control by trajectory linearization can be viewed as the ideal gain-scheduling controller designed at every point on the flight trajectory. Therefore it provides robust stability and performance at all stages of flight without interpolation of controller gains and eliminates costly controller redesigns due to minor airframe alteration or mission reconfiguration. In this paper, a prototype trajectory linearization design for an X-33 ascent flight controller is presented along with 3-DOF and 6-DOF simulation results. It is noted that the 6-DOF results were obtained from the 3-DOF design with only a few hours of tuning, which demonstrates the inherent robustness of the design technique. It is this "plug-and-play" feature that is much needed by NASA for the development, test and routine operations of the RLV's. Plans for further research are also presented, and refined 6-DOF simulation results will be presented in the final version of the paper.

1. Introduction

The Reusable Launch Vehicle (RLV) concept is NASA's approach to reliable and affordable routine space transportation. The ultimate goal of NASA's RLV R&D efforts is to *reduce the cost of routine space flight to the level of commercial air transportation.* Initiated in July 1996, the X-33 is currently being developed by NASA and Lockheed Martin as an RLV technology demonstrator. Flight control of X-33 poses a challenge to current flight controllers due to its large attitude maneuvers from liftoff to orbit and reentry. In addition, a wide range of uncertainties in vehicle handling qualities and disturbances must be accommodated by the attitude control system. NASA MSFC is currently evaluating available robust, multivariable nonlinear control theories and techniques for application to the RLV flight control system, such as the gain-scheduled ascent flight controller designed by C. E. Hall, et. al. of the Control Systems Group in the Vehicle and Systems Development Department at MSFC [1], and a sliding mode ascent controller designed by Y. Shtessel, et. al. of the University of Alabama in Huntsville [2]. The main goal is to reduce the costs for controller design and verification cycles during the development, test and operation phases of the RLV caused by limited robustness and stability margin of current flight controllers.

Nonlinear tracking and decoupling control by trajectory linearization [3] can be viewed as the ideal gain-scheduling controller designed at every point on the flight trajectory. Therefore it provides robust stability and performance at all stages of flight without interpolation of controller gains and eliminates costly controller redesigns due to minor airframe alteration or mission reconfiguration. In this paper, a prototype trajectory linearization design for X-33 ascent flight controller is presented along with 3-DOF and 6-DOF simulation results. It is noted that the 6-DOF results were obtained from the 3-DOF design with only a few hours of tuning, which demonstrates the inherent robustness of the design technique. It is this "plug-and-play" feature that is much needed by NASA for the development, test and routine operations of the RLV's.

Plans for further research are also presented and refined 6-DOF simulation results will be presented in the final version of the paper.

2. An X-33 Ascent Controller Design

The overall controller configuration is given in Figure 1, which comprises a pseudo-inverse of the nonlinear plant that computes nominal control $\bar{\mu}$, and a linear time-varying (LTV) stabilization controller that acquires stability of the nominal (command) trajectory $\bar{\eta}$ with a state feedback control law $\tilde{\mu}$. This configuration is applied to both the attitude error feedback loop and angular rate error feedback loop.

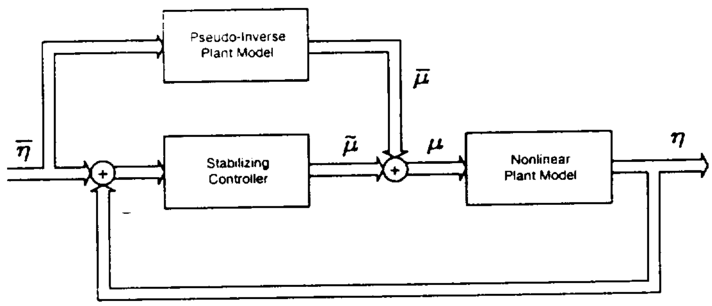

Figure 1. Nonlinear Tracking System Configuration

Integral feedback is employed for disturbance accommodation and robustness to parametric uncertainties. The attitude and rate tracking error state variables are defined, respectively, by

$$\gamma_{\text{aug}} = \begin{bmatrix} \int(\phi - \phi_{\text{com}})dt \\ \phi - \phi_{\text{com}} \\ \int(\theta - \theta_{\text{com}})dt \\ \theta - \theta_{\text{com}} \\ \int(\psi - \psi_{\text{com}})dt \\ \psi - \psi_{\text{com}} \end{bmatrix}, \qquad \omega_{\text{aug}} = \begin{bmatrix} \int(p - p_{\text{com}})dt \\ p - p_{\text{com}} \\ \int(q - q_{\text{com}})dt \\ q - q_{\text{com}} \\ \int(r - r_{\text{com}})dt \\ r - r_{\text{com}} \end{bmatrix}$$

The PI feedback control law for the attitude loop tracking error is given by $\boldsymbol{u}_1 = -\boldsymbol{K}_1(t)\gamma_{\text{aug}}$. The gain matrix where $\boldsymbol{K}_1(t)$ is calculated symbolically as

$$\boldsymbol{K}_1(t) = \begin{bmatrix} \alpha_{111} & \alpha_{112} & 0 & \bar{q}\sin(\bar{\phi}) + \bar{r}\cos(\bar{\phi}) & -\alpha_{131}\sin(\bar{\theta}) & -\alpha_{132}\sin(\bar{\theta}) \\ 0 & -\bar{r} & \alpha_{121}\cos(\bar{\phi}) & \alpha_{122}\cos(\bar{\phi}) + [\bar{q}\sin(\bar{\phi}) + \bar{r}\cos(\bar{\phi})]\sin(\bar{\phi})\tan(\bar{\theta}) & \alpha_{131}\sin(\bar{\phi})\cos(\bar{\theta}) & \alpha_{132}\sin(\bar{\phi})\cos(\bar{\theta}) \\ 0 & \bar{q} & -\alpha_{121}\sin(\bar{\phi}) & -\alpha_{122}\sin(\bar{\phi}) + [\bar{q}\sin(\bar{\phi}) + r\cos(\bar{\phi})]\cos(\bar{\phi})\tan(\bar{\theta}) & \alpha_{131}\cos(\bar{\phi})\cos(\bar{\theta}) & \alpha_{132}\cos(\bar{\phi})\cos(\bar{\theta}) \end{bmatrix}$$

where the coefficients $\alpha_{ijk}(t)$, $i = 1, 2$, $j = 1, 2, 3$, $k = 1, 2$ are obtained from the quadratic PD-eigenvalues $\rho_{ijk}(t) = -(\zeta_{ij} \pm \sqrt{1 - \zeta_{ij}^2})\omega_{nij}^2(t)$ with constant damping ζ_{ij} and time-varying bandwidth $\omega_{nij}(t)$ as follows

$$\alpha_{ij1}(t) = \omega_{nij}^2(t)$$
$$\alpha_{ij2}(t) = 2\,\zeta_{ij}\,\omega_{nij}(t) - \frac{\dot{\omega}_{nij}(t)}{\omega_{nij}(t)}$$

Similarly, the PI feedback control law for the rate loop tracking error is given by $\boldsymbol{u}_2 = -\boldsymbol{K}_2(t)\boldsymbol{\omega}_{\text{aug}}$. The gain matrix where $\boldsymbol{K}_2(t)$ is calculated symbolically by

$$\boldsymbol{K}_2(t) = \frac{1}{(g_n^p\, g_l^r - g_l^p\, g_n^r)} \cdot$$
$$\begin{bmatrix} -\alpha_{211} g_n^r & g_n^p(I_{pq}^r\bar{q} - dI_p^r) - g_n^r(I_{pq}^p\bar{q} + dI_p^p - \alpha_{212}) & 0 & g_n^p(I_{pq}^r\bar{p} + I_{qr}^r\bar{r}) - g_n^r(I_{pq}^p\bar{p} + I_{qr}^p\bar{r}) & \alpha_{231} g_n^p & g_n^p(I_{qr}^r\bar{q} - dI_r^r + \alpha_{232}) - g_n^r(I_{qr}^p\bar{q} + dI_r^p) \\ 0 & (2I_{pp}^q\bar{p} - I_{pr}^q\bar{r})(g_n^p g_l^r - g_l^p g_n^r)/g_m^q & \alpha_{221}/g_m^q & (dI_q^q + \alpha_{222})(g_n^p g_l^r - g_l^p g_n^r)/g_m^q & 0 & (2I_{rr}^q\bar{r} - I_{pr}^q\bar{p})(g_n^p g_l^r - g_l^p g_n^r)/g_m^q \\ \alpha_{211} g_l^r & g_l^r(I_{pq}^p\bar{q} + dI_p^p + \alpha_{212}) - g_l^p(I_{pq}^r\bar{q} + dI_p^r) & 0 & g_l^r(I_{pq}^p\bar{p} + I_{qr}^p\bar{r}) - g_l^p(I_{pq}^r\bar{p} + I_{qr}^r\bar{r}) & -\alpha_{231} g_l^p & g_l^r(I_{qr}^p\bar{q} - g_l^r dI_r^p) - g_l^p(I_{qr}^r\bar{q} + dI_r^r + \alpha_{232} \end{bmatrix}$$

where the parameters g_{qp}^p, etc. are functions of the time-varying moment of inertia matrix, and the over-bar indicates nominal attitude and rate.

3. Implementation and Simulation

The controller was first implemented in MATLAB with a 3-DOF simulation that included 4th-order actuator dynamics, actuator delay of 0.02 seconds, sensor delay of 0.01 seconds, sloshing and a typical wind disturbance (see Figure 2h). The closed-loop PD-eigenvalues were assigned at $\rho(t) = -(\zeta \pm \sqrt{1-\zeta^2})\omega_n^2(t)$, where $\zeta = 0.707$ for all channels in the inner and outer loop. For the nominal design, $\omega_n(t) \equiv 2.5$ and 5.0 for all channels in the outer loop and inner loop, respectively.

Figure 2 shows the attitude and body rate errors, along with the commanded control torque and disturbance torque. It is noted that the controller applies to different trajectories without rescheduling the gains, and can tolerate -25% to $+200\%$ perturbations in the vehicle's inertia, and an additional 100% of nominal actuator and sensor delays.

The controller was then implemented in MSFC Marsyas 6-DOF simulation without alteration. The results shown in figure 3 were obtained after a few hours tuning with the closed-loop bandwidth reduced to $\omega_n(t) \equiv 0.4$ and 2.5 for all channels in the outer loop and inner loop, respectively. This "plug-and-play" capability is a clear advantage of the design method.

4. Summary and Conclusions

A salient feature of the proposed control technique is that it treats nonlinear, time-varying dynamics as such and copes with it using a combination of proven and emerging nonlinear control theory and techniques and a novel spectral theory developed by the author for LTV systems. Moreover, it does not treat time-varying dynamics as a nuisance in control design, but rather makes use of it to achieve control performance and dynamic behavior beyond the reach of time-invariant controllers. It also allows in-flight tradeoff in mission objectives such as agility versus robustness. Unlike current LTI based flight controllers which treat *known* time-varying dynamics due to *nominal* flight conditions as "uncertainties," the proposed controller is capable of coping with these nominal time-varying dynamics, thereby reducing the model uncertainty that must be handled by the controller to the minimum.

The combination of our nonlinear pseudo-inversion and the LTV eigenstructure assignment controller allows one controller design for a family of plants with similar model structures. This salient feature, together with the guaranteed stability by the LTV spectral synthesis, would eliminate trial-and-error design iterations and simulation validations that are typical with GS designs. This "plug-and-play" capability would significantly shorten the design and redesign cycles, enhance availability and reliability, thereby improving affordability.

Future research plans include improving the 6-DOF performance by tuning the command shaping filter and designing a torque tracking loop. Further improvement could also come from a single loop design, at the cost of significantly more complex symbolic computations. The design method should also be applied to the descent flight controller, which is more challenging due to the limited control authority during entry phase.

Acknowledgment

The LSU authors gratefully acknowledge the guidance and support provided by Charles E. Hall, Don Krupp, Dr. Stephen G. Ryan and Dr. Henry B. Waites (retired) of the Control Systems Group in the Vehicle and Systems Development Department at NASA Marshall Space Flight Center during their 1999 NASA/ASEE Summer Faculty Fellow and Graduate Student Research Program where this research was performed.

References

[1] C. E. Hall, M. W. Gallaher, N. D. Hendrix, "X-33 Attitude Control System Design for Ascent, Transition and Entry Flight Regimes," *Proceedings of AIAA GNC Conference,* Boston, MA, August, 1998.

[2] Y. B. Shtessel, M. Jackson and C. E. Hall, "Sliding Mode Control of the X-33 Vehicle in Launch Mode," *Proceedings of 1998 American Control Conference,* June 1998.

[3] J. Zhu, *Nonlinear Tracking and Decoupling by Trajectory Linearization*, Lecture Note, Presented at NASA Marshall Space Flight Center, 137 pp., June 1998.

(More references will be provided in the complete paper.)

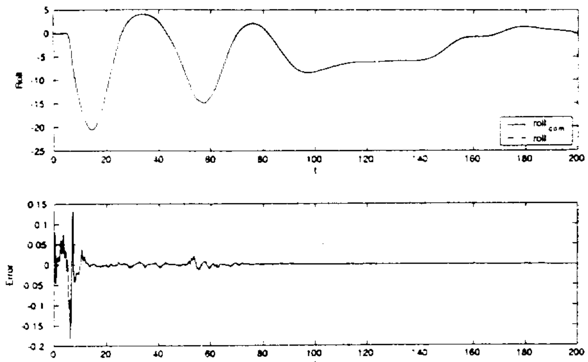

(a) Roll Tracking (deg)

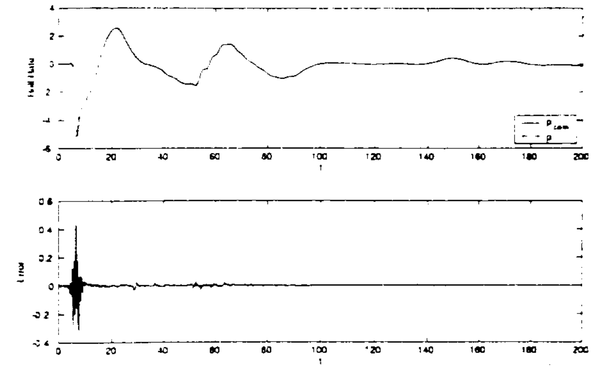

(b) Roll Rate Tracking (deg/sec)

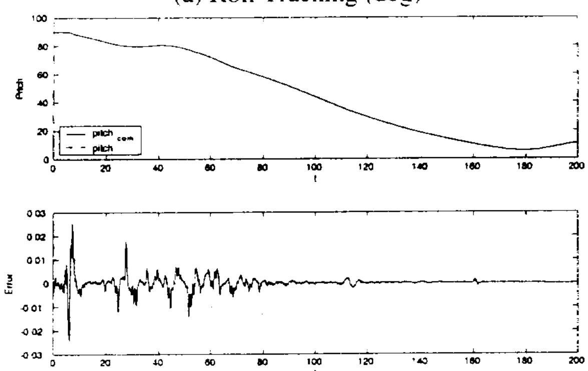

(c) Pitch Tracking (deg)

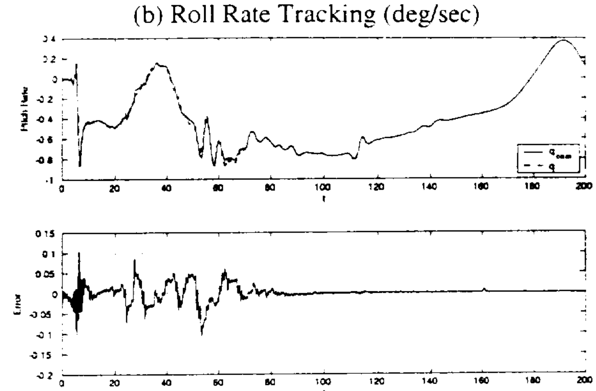

(d) Pitch Rate Tracking (deg/sec)

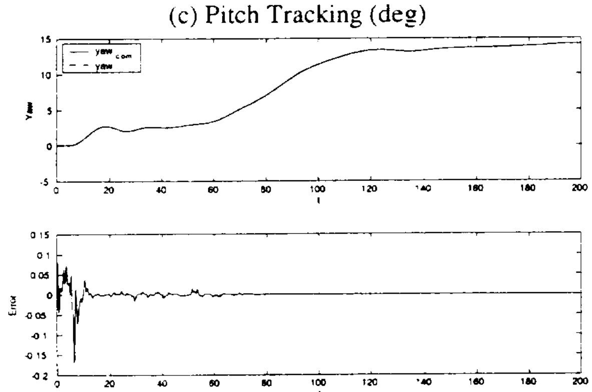

(e) Yaw Tracking (deg)

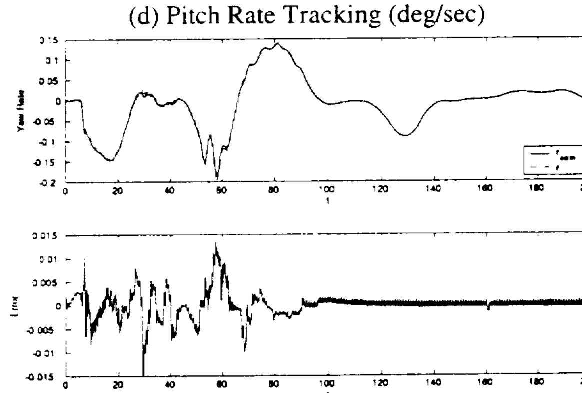

(f) Yaw Rate Tracking (deg/sec)

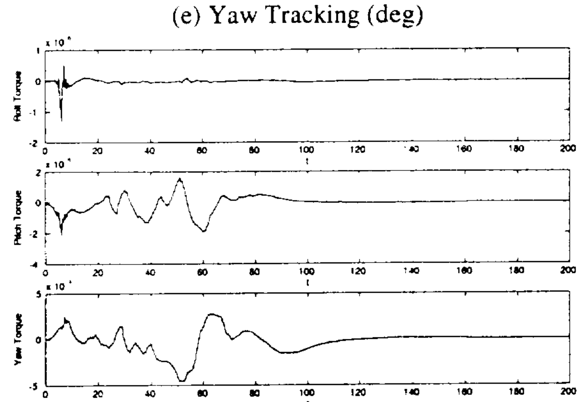

(g) Control Torque (N-m)

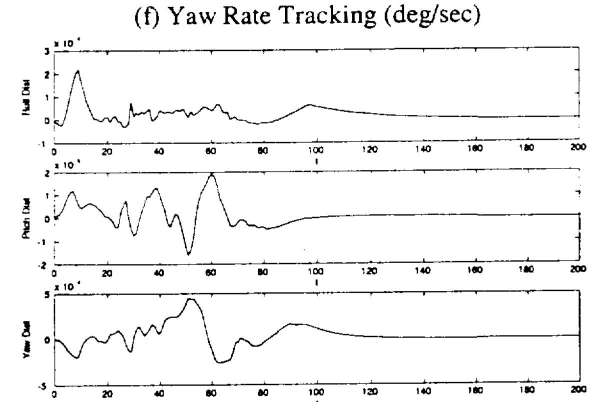

(h) Disturbance Torque (N-m)

Figure 2. 3-DOF Simulation Plots

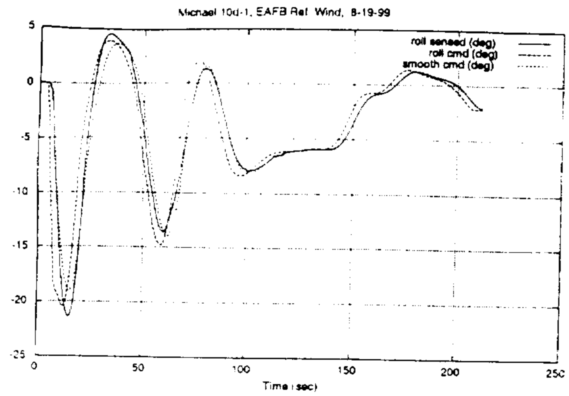

(a) Roll Tracking (deg)

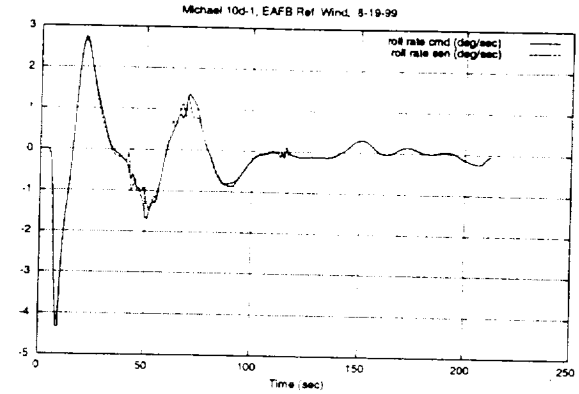

(b) Roll Rate Tracking (deg/sec)

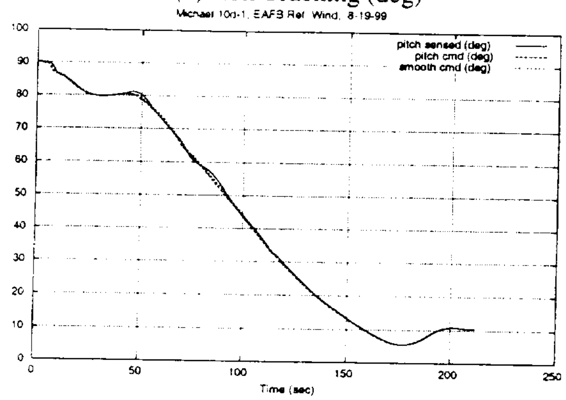

(c) Pitch Tracking (deg)

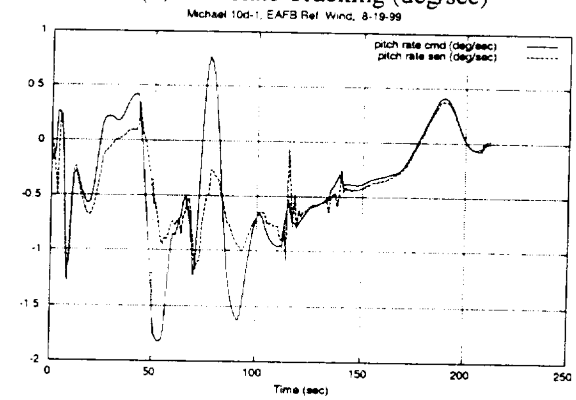

(d) Pitch Rate Tracking (deg/sec)

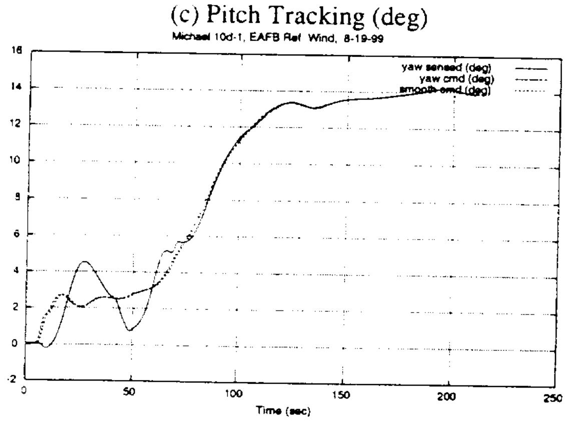

(e) Yaw Tracking (deg)

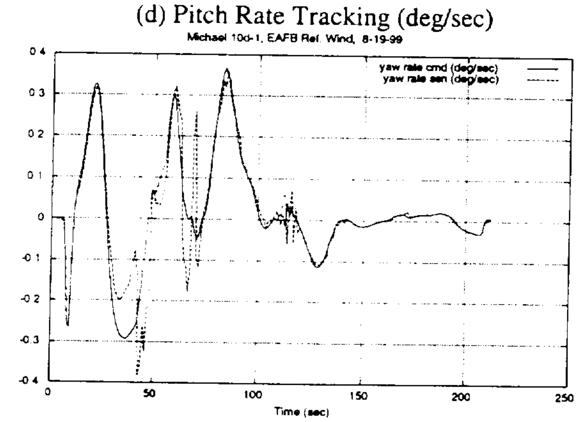

(f) Yaw Rate Tracking (deg/sec)

Figure 3. 6-DOF Simulation Plots